ELSEVIER

Thermochimica Acta 342 (1999) 167–174

thermochimica acta

www.elsevier.com/locate/tca

Synthesis of stoichiometric cadmium substituted magnetites and formation by oxidation of solid solutions of cadmium ferrite and γ-iron oxide

B. Gillot[a,*], D. Thiebaut[a], M. Laarj[b]

[a]*Laboratoire de Recherches sur la Réactivité des Solides, UMR 5613, Université de Bourgone, CNRS BP 47870-21078 Dijon Cedex, France*
[b]*Département de Chimie, Faculté des Sciences Semlalia, B.P. S; 15, Marrakech, Morocco*

Received 10 March 1999; received in revised form 20 August 1999; accepted 20 August 1999

Abstract

Stoichiometric cadmium-substituted magnetites $Cd_xFe_{3-x}O_4$ ($x = 0$, 0.25, 0.50, 0.75 and 1) were prepared by a standard ceramic method. It has been found that, after grinding, these Cd-ferrites can be oxidized under prolonged isothermal conditions at low temperature (<300°C) whilst retaining the single spinel phase. The oxidation and the resulting non-stoichiometric solid solutions between $CdFe_2O_4$ and γ-Fe_2O_3 have been investigated by X-ray diffraction, differential scanning calorimetry, thermogravimetric analysis and infrared spectroscopy. A cation distribution for defect solid solutions of maghemite, γ-Fe_2O_3, and cadmium ferrite has been proposed.

Keywords: Cadmium ferrite; γ-Fe_2O_3; Oxidation; Grinding; Cation-deficient spinel

1. Introduction

We showed, in previous publications that only the substituted magnetites $M_xFe_{3-x}O_4$ (M = Co, Zn, Al, Cr, Mo, V) prepared at low temperatures (<500°C) with a crystallite size of about a hundred of nanometers, allow cation-deficient spinels (γ-phases) to be obtained in the presence of oxygen [1]. In contrast, the ferrites prepared at high temperature (1000°C or more) lead to the formation of large particles (several micrometers) which are unable to react without spinel phase decomposition (α-phases) because of a higher oxidation temperature [2–4].

In fact, depending on the crystallite size, the following simplified overall reactions can be observed for solid solutions MFe_2O_4–Fe_3O_4 (M = Zn, Co, Ni):

$$MFe_2O_4{-}Fe_3O_4 + O_2 \rightarrow \gamma\text{-}MFe_2O_4{-}Fe_2O_3 \quad (1)$$

for crystallite sizes below about 0.3 μm, whereas for larger particle sizes, several reactions were observed according to:

$$MFe_2O_4{-}Fe_3O_4 + O_2 \rightarrow \gamma\text{-}MFe_2O_4{-}Fe_3O_4{-}Fe_2O_3 \quad (2)$$

$$\gamma\text{-}MFe_2O_4{-}Fe_3O_4{-}Fe_2O_3 \rightarrow MFe_2O_4{-}Fe_3O_4 + \alpha\text{-}Fe_2O_3 \quad (3)$$

$$MFe_2O_4{-}Fe_3O_4 + O_2 \rightarrow MFe_2O_4 + \alpha\text{-}Fe_2O_3 \quad (4)$$

*Corresponding author. Tel.: +33-3-80-396142; fax: +33-3-80-396167
E-mail address: bgillot@satie.u.bourgogne.fr (B. Gillot)

0040-6031/99/$ – see front matter
PII: S0040-6031(99)00310-X

Reaction (2) represents oxidation for particle sizes of about 1 μm and reaction (4) oxidation for particle sizes of about 10 μm. This result is associated with increased particle size which causes α-Fe_2O_3 to precipitate during oxidation [4].

Some studies on the cadmium ferrites aim as is to prepare stoichiometric Cd-substituted magnetites, $Cd_xFe_{3-x}O_4$ $(0 \leq x \leq 1)$ [5,6] at low temperature by wet methods have indicated a very narrow range of temperature and of duration of thermal treatment favorable to the formation of these nanosized ferrites. For such solid solutions and their corresponding non-stoichiometric $xCdFe_2O_4$–$(1-x)\gamma$-Fe_2O_3 spinel phases, the x values remain low ($x \leq 0.3$). Thereby, only can be studied oxidized solid solutions with a high vacancies content. On the other hand our attempt to prepare pure stoichiometric and non-stoichiometric $Cd_xFe_{3-x}O_{4+\delta/2}$ spinels using soft chemistry methods in the whole $0 \leq x \leq 1$ region also has been unsuccessful because thermal treatments lead to a very complex system of non-stoichiometric solid solutions. Only ultrafine particles of cadmium ferrite, $CdFe_2O_4$, have been prepared by a coprecipitation method [7].

In this paper, the formation at moderate temperature of stoichiometric cadmium ferrites $Cd_xFe_{3-x}O_4$ $(0 \leq x \leq 1)$ by a standard ceramic route is investigated. The most favorable conditions, as for example the grinding time and the oxidation temperature, for obtaining non-stoichiometric $Cd_xFe_{3-x}O_{4+\delta/2}$ spinels without the presence of foreign phases have been defined.

2. Samples and analytical methods

The $Cd_xFe_{3-x}O_4$ samples with $x = 0$, 0.25, 0.50, 0.75 and 1 were prepared by manual grinding in an agate mortar of appropriate proportions of powdered cadmium (II) oxide, α-iron (III) oxide (Aldrich, spec-pure grade) and metallic iron. The well-homogenized powder was put into an alumina crucible placed inside a silica ampule. The ampule was then degassed under vacuum (10^{-8} Pa) in order to avoid, for $x < 1$, oxidation at high temperature of Fe^{2+} ions, sealed and heated between 900°C and 980°C (Table 1), afterwards it was quenched in water. The grinding and firing operations were repeated at least once. To verify the possible loss of cadmium, which is volatile above 900°C, a sample with $x = 0.50$ was analyzed for different firing temperatures (Table 1). As a result of thermal treatment in a vacuum above 930°C, the loss of cadmium leads to a lattice parameter lower compared with a stoichiometric sample (Table 1). Thereby, for each composition, the most favorable conditions have been determined to avoid the loss of cadmium, the final product with the higher parameter being checked by X-ray diffraction. Thus, by firing at lower temperatures and for short periods compared to the previous studies [8,9], cadmium volatilization is suppressed and stoichiometric samples can be obtained.

X-ray diffraction powder patterns were taken at room temperature using a Siemens D-5000 diffractometer operating in the reflexion mode with CuK_α radiation at a scanning rate of $0.003^\circ\ s^{-1}$. The scanning range was $25^\circ < 2\theta < 80^\circ$ and the experimental values of the lattice parameter for the spinel structure in the investigated samples were obtained by least-squares refinement. The percentage of cadmium was analyzed by atomic absorption spectroscopy after dissolving the sample powder in a concentrated HCl solution (Table 1). The grain sizes before and after

Table 1
Characteristics of stoichiometric $Cd_xFe_{3-x}O_4$ spinels

x value (sample $Cd_xFe_{3-x}O_4$)	Preparation temperature (°C)	Cd (wt%)		Average particle size (μm)	Surface area (m^2/g)	Lattice parameter (nm)
		Experimental	Theoretical			
0	980	0	0	5	1.9	0.8396
0.25	950	11.44	11.45	4	2.7	0.8485
0.50	930	21.63		6	1.5	0.8556
	950	21.20	21.63	6	1.5	0.8538
	960	20.80		7	1.2	0.8522
0.75	930	30.75	30.77	6	1.5	0.8631
1	900	39.02	39.01	8	1	0.8698

grinding, reported in Table 1, are determined by measurements of surface areas with a Quantachrome Autosorb 1.

The oxidations were performed with the temperature increasing linearly (2.5°C min^{-1}) or under isothermal conditions in a Setaram TG 24 microbalance (symmetrical set-up, resolution and noise level 0.1 μg) using 15 mg of powder. The degree of oxidation at various levels of reaction was calculated from the gravimetric data.

FT-IR spectra were recorded in air at room temperature with a Perkin-Elmer 1725X instrument over the range 4000–450 cm^{-1} and with a Perkin-Elmer 1700 instrument over the range 450–50 cm^{-1}. Transmittance spectra were obtained on 1 mg of powdered sample dispersed in 200 mg of CsI pellets pressed under vacuum at 10 Pa. The calorimetric analyzes were performed at 10°C min^{-1} heating rate using 60 mg of powder in a Setaram DSC 111G.

3. Results and discussion

3.1. Unoxidized samples

X-ray diffraction patterns are shown in Fig. 1 and the values of the lattice parameter are presented in Table 1. The parameters for magnetite ($x = 0$) and cadmium ferrite ($x = 1$) are in good agreement with the reported one [10,11]. Fig. 2a (curve 1) shows the relation between the composition and lattice parameter. From this figure, one can clearly see that the lattice parameter strongly increases with increasing cadmium content. Curve 3 shows for $x \leq 0.3$ a similar behavior for Cd-ferrites prepared by a ceramic sintering method where the lattice parameter increases from 0.8396 ($x = 0$) to 0.8506 nm ($x = 0.3$) [8]. This could be due to the large ionic radius of Cd^{2+} (0.092 nm), which when substituted in the lattice, resides on an A-site and displaces the smaller Fe^{3+} ion (0.065 nm) from an A- to a B-site. Along with shifts in the peak positions, the transition from inverse to normal structure with increasing cadmium causes changes in relative peak intensities, most apparent for the 220 and 422 reflexions (Fig. 1) which are mostly sensitive to cations on tetrahedral sites. The intensities of these peaks increase with increasing Cd^{2+} content. It can thus be considered that $CdFe_2O_4$ has a normal spinel

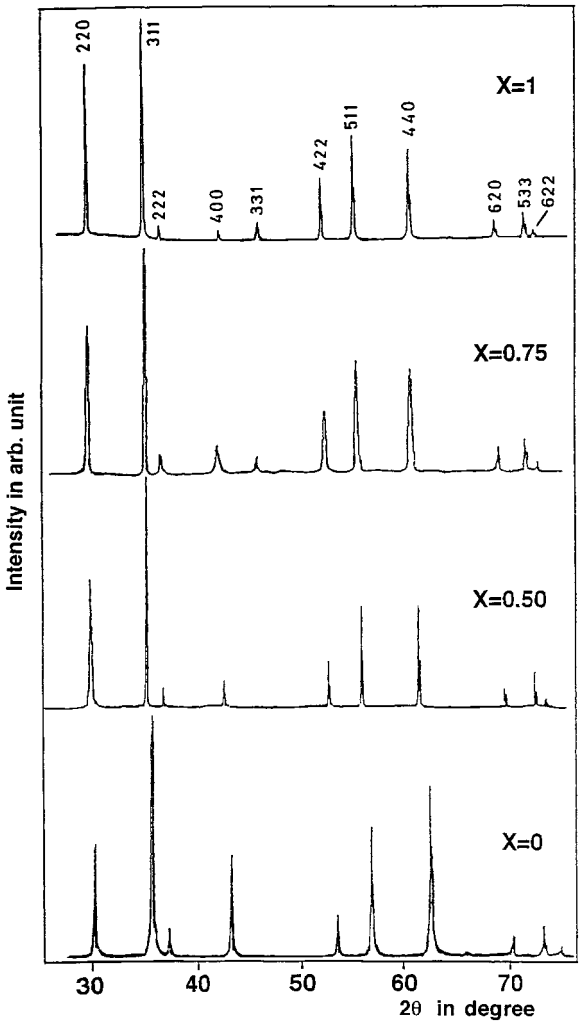

Fig. 1. X-ray diffraction pattern of stoichiometric $Cd_xFe_{3-x}O_4$ spinels.

structure in which tetrahedral A-sites are occupied by Cd^{2+} ions and octahedral B-sites by Fe^{3+} ions while it has long been known that Fe_3O_4 has an inverse spinel structure in which B-sites are occupied both by Fe^{2+} and Fe^{3+} ions. Thus, for the series of solid solutions between $CdFe_2O_4$ and Fe_3O_4, a cation distribution can be predicted as:

$$(Cd_x^{2+} \quad Fe_{1-x}^{3+})_A(Fe_{1-x}^{2+} \quad Fe_{1+x}^{3+})_B O_4^{2-} \qquad (5)$$

To confirm this distribution, lattice parameters were also calculated using the equations developed by Poix [12,13] and based on the invariant character of metal–

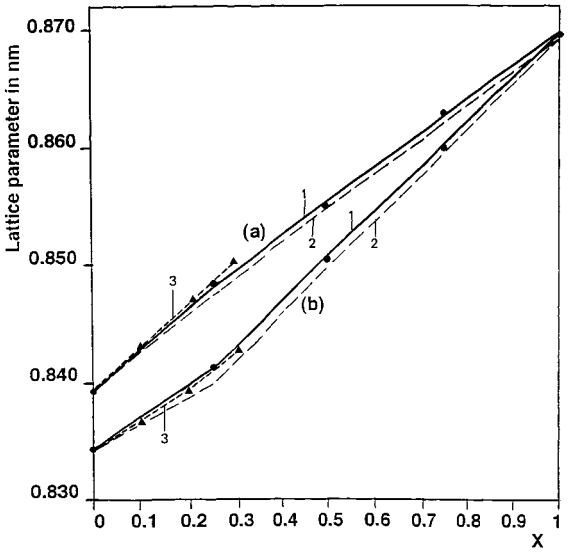

Fig. 2. Evolution of lattice parameter versus cadmium content: (a) stoichiometric spinels — (1) experimental; (2) calculated curve assuming formula (5) and Eq. (6); (3) from Ref. [8]. (b) Non-stoichiometric spinels — (1) experimental; (2) calculated curve assuming formula (9) and Eq. (6); (3) from Ref. [17].

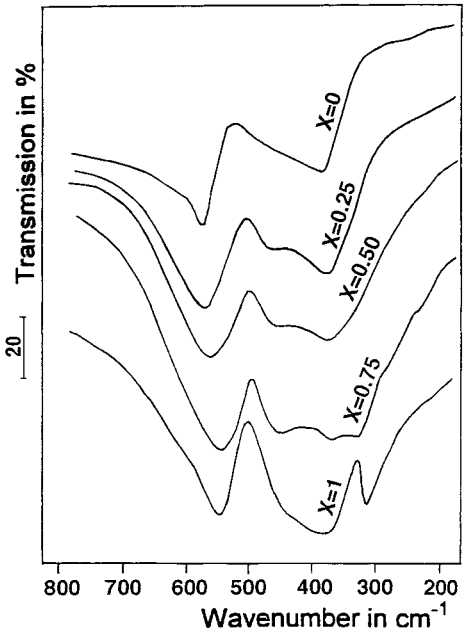

Fig. 3. FT-IR spectra of stoichiometric $Cd_xFe_{3-x}O_4$ spinels.

oxygen distances listed in Table 2. The parameter is given by the equation:

$$a = 2.0995 d_A + (5.8182\, d_B^2 - 1.4107\, d_A^2)^{1/2}. \quad (6)$$

As shown in Fig. 2a (curve 2), the calculated curve for the distribution (5) is in a reasonable agreement with the experimental curve. Other distributions, as for example Cd^{2+} ions at B-sites, do not agree with this distribution. However, as shown in Fig. 2, the calculated lattice parameters (curve 2) were systematically lower than those observed (curve 1). These small differences can be attributed to the possibility of some cation disorder. For $x = 0$, Otero Arean et al. [14] for cadmium–zinc ferrites and Yokoyama et al. [7] for ultrafine particles of cadmium ferrite have found a deviation of the cation distribution from the normal spinel structure suggesting a partially octahedrally occupancy of the Cd^{2+} ions.This cation distribution is in part confirmed by the infrared spectra. It appears from Fig. 3 that the spectrum of $CdFe_2O_4$ shows three pronounced absorption bands occurring at $\upsilon_1 = 543\ cm^{-1}$, $\upsilon_3 = 376\ cm^{-1}$ and $\upsilon_4 = 315\ cm^{-1}$. Over the range examinated the spectrum of Fe_3O_4 consists only of two prominent absorption bands $\upsilon_1 = 578\ cm^{-1}$ and $\upsilon_3 = 378\ cm^{-1}$. Also, the spectrum shows for $0 < x < 1$ a weak absorption band υ_2 at about $450\ cm^{-1}$. It has been reported previously that for a spinel-type oxide with space group Fd3m-Oh [15,16], the high frequency band υ_1 is belonging to the tetrahedral site and the low frequency band υ_3 to the octahedral complexes. Fig. 4 displays the variation of the position of the bands with the cadmium content. It can be seen that both the frequency υ_1 is strongly shifted to lower frequencies as the cadmium content increases while the υ_3 band is almost constant. This indicates that, unlike the octahedral sites, the cation distribution in the tetrahedral sites is strongly modified. Indeed, the substitution of cadmium in A-sites is associated with the decrease in the bond stretching

Table 2
Cation–oxygen distances used to calculate the theoretical value of the lattice parameter[a]

Metal–oxygen bonds	A-site (nm)	B-site (nm)
Fe^{2+}–O	0.2003	0.2132
Fe^{3+}–O	0.1858	0.2020
Cd^{2+}–O	0.2169	0.2347
□–O	0.2078	0.2240

[a] The bond lengths come from Ref. [12,13].

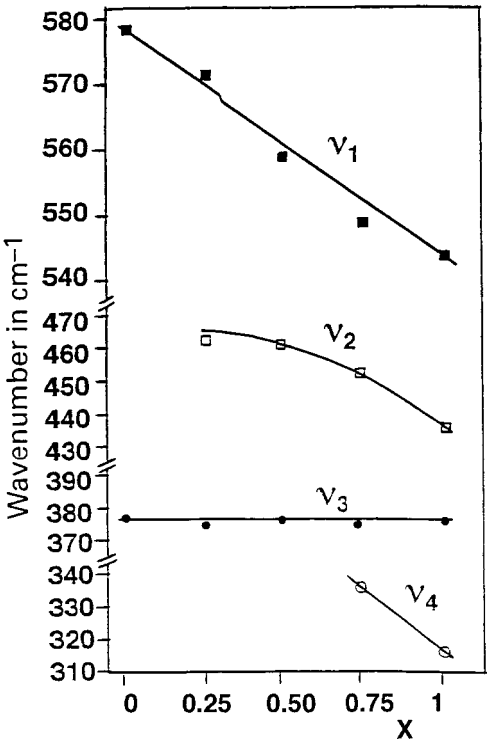

Fig. 4. Compositional dependence of absorption frequencies bands of $Cd_xFe_{3-x}O_4$ with cadmium content.

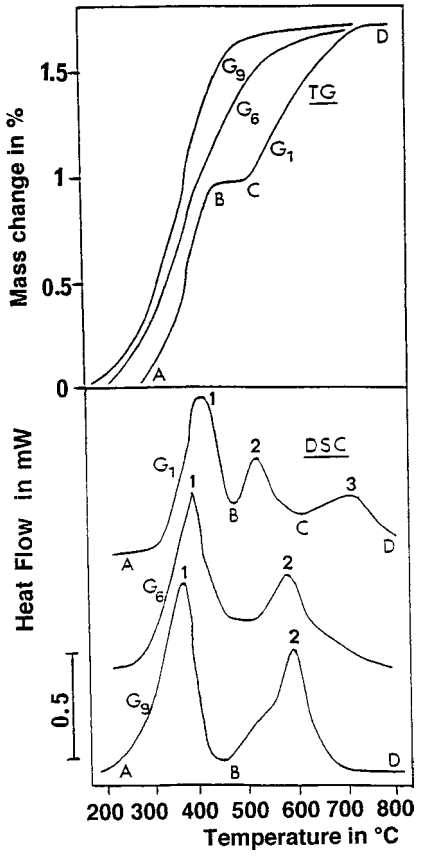

Fig. 5. DSC and TG curves for oxidation in air of a $Cd_{0.5}Fe_{2.5}O_4$ spinel ground for 1 (G_1), 6 (G_6) and 9 min (G_9). Peaks 1 and 2 represent oxidation and precipitation, respectively, and peak 3 represent oxidation of residual Fe_3O_4.

force constant of these sites which is exhibited in the increase of bond lengh of the A-sites as confirmed by the increase of the lattice parameter.

3.2. Oxidized samples: Requirement to obtain solid solutions of $CdFe_2O_4$ and γ-Fe_2O_3

In order to enhance the reactivity, the stoichiometric spinels were submitted to dry grinding under N_2 for different time periods. The grain size decreases as the time of grinding increases and for samples ground for 1 (sample G_1), 6 (sample G_6) and 9 min (sample G_9), particle sizes determined by SEM were about 4, 1 and 0.5 μm, respectively. As an example, Fig. 5 shows the effect of particle size on oxidation behavior of a $Cd_{0.5}Fe_{2.5}O_4$ spinel. As revealed by DSC curves, three exothermic peaks were observed for sample G_1 and only two peaks for samples G_6 and G_9. During the DSC runs the samples are quenched in air from the temperatures corresponding to points B, C and D. For sample G_1 and in the region AB where an increase in mass is observed in the TG curve, the XRD analysis reveals that the spinel structure is maintained as the lattice parameter decreases, indicating solid solutions formation consistent with reaction (2). In the region BC (reaction 3), we have, in addition to the spinel phase, the precipitation of α-Fe_2O_3. Evidently, this results from decomposition of the γ-Fe_2O_3 formed in reaction (2) since the second exothermic effect is not accompanied by a change of mass (Fig. 5). In the region CD, we again observe a continuous mass gain in the TG curve due to further oxidation of the Fe^{2+} ions still present in the solid solution. However, high-temperature oxidation causes the formation of α-Fe_2O_3 and $CdFe_2O_4$ according to reaction (4).

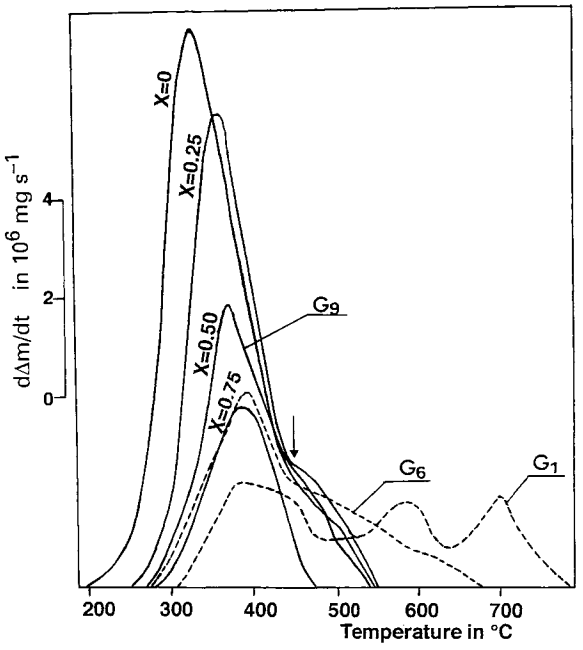

Fig. 6. DTG curves of samples heated in pure O_2 ($PO_2 = 2 \times 10^4$ Pa) at a linear rate of 2°C min^{-1}; (——) samples ground for 9 min (G9), (——) $Cd_{0.5}Fe_{2.5}O_4$ ground for 1 (G_1) and 6 min (G_6).

For samples G_6 and G_9 with lower particle sizes, the two exothermic peaks (Fig. 5) can be assigned from X-ray analysis to reactions (2) and (4). The mass gain takes place in a single step and for the region AB, the oxidation reaction for sample G_9 is almost complete at ca. 500°C and shows no evidence for conversion of the α-Fe_2O_3 structure. Examination of the DTG curves (Fig. 6) for a sample ground 9 min confirms an oxidation process in one stage associated with the oxidation of Fe^{2+} ions on B-sites [3] when the reaction was completed at 540°C. Moreover the anomaly in oxidation rate at 450°C (marked by an arrow on Fig. 6) indicates that, above this temperature, the compound has gone beyond the stability field of spinel phase. Appearance of α-Fe_2O_3 is observed by X-ray diffraction. The decrease in peak intensity and the shifting toward higher temperatures with increasing cadmium content can be related both to the amount of Fe^{2+} ions and to the stabilizing effect of cadmium. For G_1 and G_6 samples, considerable variations occurred and for G_1 two other broad pronounced peaks were observed although Fe^{2+} ions remain located on B-sites. These peaks are associated with the oxidation of the remaining Fe^{2+} ions [3]. These observations, together with a significant decrease in the lattice parameter (the lattice parameter decreases from 0.8556 to 0.8511 nm) allows us to enlarge the upper limit of the field of existence of defective solid solutions $CdFe_2O_4$ and γ-Fe_2O_3.

The DSC and DTG results were used to select oxidation conditions for the formation of defect solid solutions obtained from stoichiometric $Cd_xFe_{3-x}O_4$ spinels in the case of G_9 samples according to the reaction:

$$Cd_xFe_{3-x}O_4 + \delta/2O_2 \quad \rightarrow \quad Cd_xFe_{3-x}O_{4+\delta/2} \tag{7}$$

The initial and final temperatures for reaction (7) are taken in the range 290–250°C depending on composition. Hence, in order to obtain non-stoichiometric spinels without α-Fe_2O_3 precipitation, the samples were held isothermally at different temperatures for various oxidation times (Table 3). XRD patterns (Fig. 7) reveal the single-phase spinel structure without any ambiguous reflexion. For $x = 0$ and 0.25, the diffraction lines were very broad indicating

Table 3
γ and lattice parameter values of solid solutions obtained by oxidation of the $Cd_xFe_{3-x}O_4$ spinels

x value (sample $Cd_xFe_{3-x}O_{4+\delta/2}$)	Oxidation conditions (sample G_9)		$\delta/2$ (theoretical)	$\delta/2$ (G_9)	Number of vacancies per molecule	Lattice parameter (nm)
	T (°C)	Time (h)				
0	290	17	0.500	0.493	0.328	0.8341
0.25	250	14	0.375	0.372	0.255	0.8413
0.50	250	15	0.250	0.250	0.176	0.8502
0.75	270	17	0.125	0.124	0.090	0.8591
1	270	14	0	0	0	0.8698

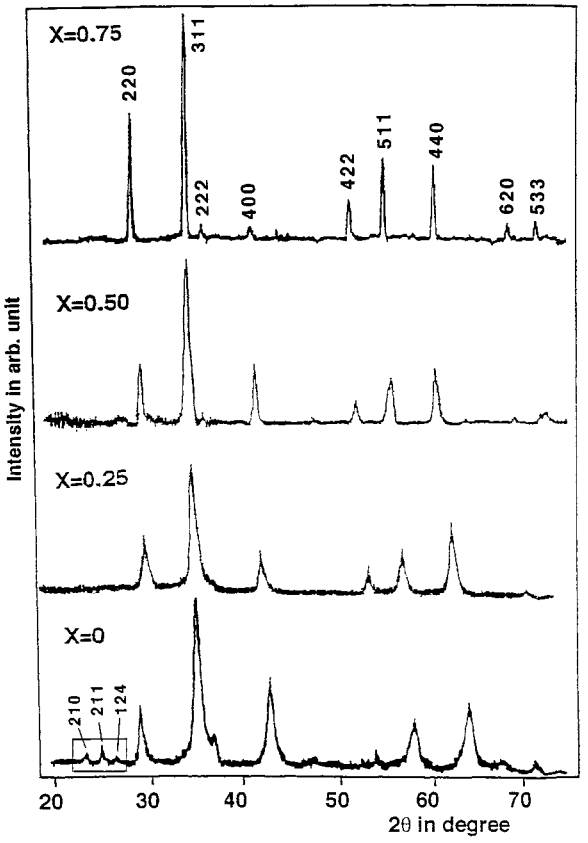

Fig. 7. X-ray diffraction pattern of oxidized $Cd_xFe_{3-x}O_{4+\delta/2}$ spinels.

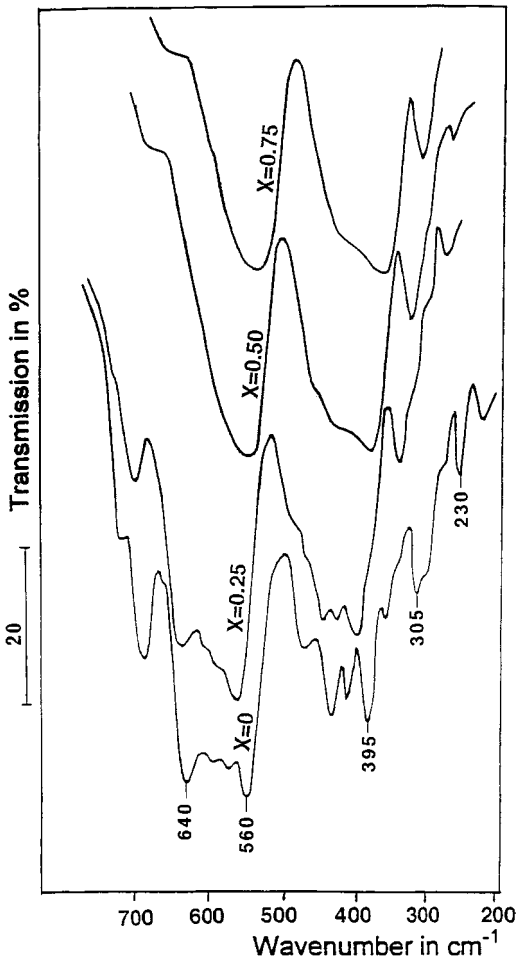

Fig. 8. FT-IR spectra of oxidized spinels.

both the existence of small crystallite sizes consequent to grinding and the presence of vacancies which causes more broadening than the "chemical" disorder resulting from having Fe^{2+} and Fe^{3+} on equivalent sites. Moreover, for $x = 0$, the diffractogram evidences the presence in the low angle region of extra reflexions forbidden in the space group Fd3m and indicating some degree of order in the vacancies distribution [17]. The values of the lattice parameter are presented in Table 3. The lattice parameter increases nearly linearly with increasing cadmium content (Fig. 2b, curve 1). A similar evolution was observed by Ito et al. [18] for completely oxidized Cd(II)-bearing ferrites for $x \leq 0.3$ (Fig. 2b, curve 3) which form a limited solid solution between γ-Fe_2O_3 and $CdFe_2O_4$.

On the basis of the FT-IR spectra (Fig. 8), there is also an indication of presence of vacancies on B-sites, at least for $x = 0$ and 0.25, where a relatively high number of absorption bands are observed; we have established [19] that this fine structure corresponds to an ordering of the vacancies and cations distributed on octahedral sites. With increase of cadmium content, the number of absorption bands decreases and the spectrum is only slightly different from that of the unoxidized spinels of the same composition. This results because of a lower amount of vacancies in the B-sites formed by oxidation of Fe^{2+} ions.

For such cation deficient spinels, the mass gain measured after complete oxidation corresponds to the number of added oxygen atoms $\delta/2$ (Table 3) and is linked to the number δ of exchanged electrons

between O^{2-} anions and Fe^{2+} ions. In order to keep the structural unit to four oxygen atoms, it is necessary to introduce vacancies in the spinel lattice. The vacancies number, ($\square$) depends on the number of exchanged electrons δ and the cation deficient spinel may be written as:

$$\left(\mathrm{Cd}^{2+}_{8x/8+\delta} \quad \mathrm{Fe}^{3+}_{24-8x/8+\delta} \quad \mathrm{squarebox}_{3\delta/8+\delta}\right)\mathrm{O}^{2-}_4$$
$$\text{with } \delta = 1-x.$$

Since it was suggested that the Cd^{2+} ions occupy only the A-sites and the vacancies of the B-sites, the cation distribution between A- and B-sites becomes:

$$\left(\mathrm{Cd}^{2+}_{8x/9-x} \quad \mathrm{Fe}^{3+}_{9(1-x)/9-x}\right)_{\mathrm{A}} \times \left(\mathrm{Fe}^{3+}_{15+x/9-x} \quad \mathrm{squarebox}_{3(1-x)/9-x}\right)_{\mathrm{B}} \mathrm{O}^{2-}_4.$$

A fairly good agreement was obtained between the experimental lattice parameter determined for $CdFe_2O_4$–γ-Fe_2O_3 solid solutions and then calculated by the Poix method, assuming the vacancies to be located in the octahedral sites and the tetrahedral sites to be occupied by cadmium cations (Fig. 2b, curve 2). This distribution is however somewhat different from that evaluated by the cluster component method by Firsov and Popov [20] that found that an amount of cadmium ions (20%) occupied octahedral sites.

References

[1] B. Gillot, A. Rousset, HCR Comprehensive Review 1 (1994) 69.
[2] B. Gillot, A. Rousset, G. Dupré, J. Solid State Chem. 25 (1978) 263.
[3] B. Gillot, B. Domenichini, Mater. Chem. Phys. 47 (1997) 217.
[4] T. Kimura, S. Ohishi, T. Yamaguchi, J. Am. Ceram. Soc. 62 (1979) 533.
[5] K. Keneko, T. Takei, Y. Tamaura, T. Kanzaki, T. Katsura, Bull. Chem. Soc. Jpn. 47 (1974) 1646.
[6] W. Wolski, E. Wolska, J. Kaczmarek, J. Solid State Chem. 110 (1994) 70.
[7] M. Yokoyama, E. Ohta, T. Sato, J. Magn. Magn. Mater. 183 (1998) 173.
[8] H.N. Ok, B.J. Evans, Phys. Rev. 14B (1976) 2956.
[9] Z. Panek, K. Fitzner, Thermochim. Acta 66 (1983) 127.
[10] B.A. Wechsker, D.H. Lindsley, C.T. Prewitt, Am. Mineral 69 (1984) 754.
[11] A.A. Ghani, A.A. Sattar, J. Pierre, J. Magn. Magn. Mater. 97 (1991) 141.
[12] P. Poix, Bull. Soc. Chim. Fr. 5 (1965) 1085.
[13] P. Poix, C.R. Acad. Sci. 268 (1969) 1139.
[14] C. Otero Arean, E. Garcia Diaz, J.M. Rubio Gonzalez, M.A. Villa Garcia, J. Solid State Chem. 77 (1988) 275.
[15] W.B. White, B.A. DeAngelis, Spectrochim. Acta A23 (1967) 985.
[16] S.A. Mazen, N.A. Hakeem, B.A. Sabrah, Phys. Stat. Sol. (B) 123 (1984) K1.
[17] C. Greaves, J. Solid State Chem. 49 (1983) 325.
[18] K. Ito, Y. Tamaura, T. Katsura, Bull. Chem. Soc. Jpn. 57 (1984) 2820.
[19] B. Gillot, Vibrational Spectroscopy 6 (1994) 127.
[20] P.Yu. Firsov, G.P. Popov, Russ. J. Phys. Chem. 55 (1981) 344.